Article No. mb981962 *J. Mol. Biol.* (1998) **281**, 675–687

JMB

Molecular Dynamics Simulations of an Oligonucleotide Duplex with Adenine Tracts Phased by a Full Helix Turn

M. A. Young and D. L. Beveridge*

Chemistry Department and Molecular Biophysics Program Wesleyan University Middletown CT 06459, USA

A theoretical model of a DNA oligonucleotide duplex featuring A-tracts phased by a full helix turn is developed based on molecular dynamics computer simulation. The extent to which this model agrees with relevant experimental data on axis bending and the relationship of A-tracts to bending and other aspects of helix morphology is investigated. Specifically, a series of nanosecond-level molecular dynamics (MD) simulations have been carried out for the 25 bp duplex d(ATAGGCAAAAAATAGGCAAAAATGG) at various concentrations of saline solution. A 30 base-pair sequence composed of three 10 bp repeats of the *Bam*HI recognition sequence ligated together, d(CGGGATCCCG·CGGGATCCCG·CGGGATCCCG), was simulated as a control. The MD was carried out using the AMBER 4.1 suite of programs, and utilized the Cornell *et al*. force-field with the electrostatic boundary conditions treated by the particle-mesh Ewald summation protocol. The MD results show that at a concentration of 60 mM KCl, 10 mM $MgCl_2$ added salt plus minimal neutralizing cations, the MD model exhibits concerted axis bending to the extent of 15.5° per A-tract. This compares favorably with the bending per turn of 17 to 21° inferred from cyclization experiments. The MD model also exhibits a progressive 5′ to 3′ narrowing of the minor-groove region of A-tracts, a feature inferred from DNA footprinting experiments. Analysis of the dynamic structure of the MD models shows that the origin of the bending follows a junction-type bending model with an admixture of mixed sequence effects, with A-tracts relatively straight, as in oligonucleotide crystal structures of sequences containing A-tracts. The results are shown to be sensitive to environmental conditions: MD on d(ATAGGCAAAAAATAGGCAAAAATGG) in neutralizing Na^+ buffer results in markedly reduced curvature, and the removal of Mg^{2+} measurably affects bending. Carrying out the simulations at experimental salt conditions appears to be essential to obtain an accurate account of the experimentally observed bending.

Keywords: DNA bending; persistence length; A-tracts; molecular dynamics; magnesium

**Corresponding author*

Introduction

The effect of phased A-tracts on oligonucleotide duplex structure is a most important and well-documented example of DNA sequence effects. The behavior of proposed theoretical models of DNA involving A-tracts is of considerable significance in assessing the credibility of a proposed nucleic acid force and in developing an explanation of the structural effects of A-tracts at the molecular level. We describe a project in which a dynamical model of a DNA featuring phased A-tracts is obtained using molecular dynamics (MD) computer simulation, and investigate (a) the extent to which this model agrees with relevant experimental data on this sequence motif, and (b) how the

Abbreviations used: MD, molecular dynamics; CAP, catabolite gene activator protein; TBP, TATA box binding protein; MPD, methylpentane diol; PME, particle mesh Ewald; rms, root-mean-square; rmsd, root-mean-square deviation.

E-mail address of the corresponding author: dbeveridge@wesleyan.edu

0022–2836/98/340675–13 $30.00/0

dynamic model corresponds to current hypotheses about the relationship between A-tracts and DNA bending. MD studies of the 25 bp oligonucleotide of sequence d(ATAGGCAAAAAATAGGCAAAAATGG) with a full complement of solvent water and counterions have been carried out. This sequence features two successive A-tracts spaced by 11 bp in the sequence, in phase with a full turn of a *B*-form double helix. This sequence is referred to also as the phased A-tract sequence. The MD simulations consider a range of counterion concentrations commensurate with experimental conditions, and are extended into the nanosecond regime of time. A corresponding sequence composed of three repeats of the *Bam*HI recognition sequence, d(CGGGATCCCGCGGGATCCCGCGGGATCCCG), commonly employed as a marker in gel migration experiments and lacking in phased A-tracts, is studied as a control. No specific assumptions with respect to DNA bending, the behavior of A-tracts, or helix morphology *per se* have been introduced into the MD simulation.

Background

The effect of DNA sequence on structure is a matter of central concern in the understanding of the structural biology and functional energetics of informational macromolecules (Saenger, 1983). One of the earliest observed and most notable instances of sequence effects on structure occurs in nucleosomal DNA, in which two turns of DNA are supercoiled around an octamer of histone proteins in the fashion of a solenoidal wrap (Luger *et al*., 1997; Sinden, 1994). The base-pair sequence of the DNA in nucleosomes was found to have a distinct feature: stretches of consecutive adenine nucleotides (A-tracts) spaced by the number of base-pairs in a full turn of the *B*-form DNA duplex (Ioshikhes *et al*., 1992; Shrader & Crothers, 1990). A hypothesis subsequently emerged that bending or bendability is linked in some way to the individual A-tracts in DNA sequences, and that the phasing of A-tracts by a full helical in a DNA duplex serves to constructively amplify the effect in a concerted direction.

A causal link between A-tracts and DNA bending has been supported by a number of experiments on DNA oligonucleotides of lengths ranging from around just over one helical turn, to hundreds of base-pairs (for a review, see Hagerman, 1990). The experimental evidence for the curvature of A-tracts was originally observed in the minicircle kinetoplast DNA of trypanosomes (Marini *et al*., 1982), and is based primarily on the anomalous migration of A-tract DNA oligonucleotides on gels (Diekmann, 1987; Hagerman, 1985; Koo & Crothers, 1988), and the cyclization kinetics of DNA plasmid formation (Crothers *et al*., 1992). The A-tract effect has been employed in a novel study investigating the role of DNA bending in the mechanism of transcription regulation mediated by the DNA-bending protein catabolite gene activator protein (CAP) in both *in vivo* and *in vitro* prokaryotic systems (Bracco *et al*., 1989; Gartenberg & Crothers, 1991), and more recently in a study of the role of bending by TATA-Box Binding Protein (TBP) in eukaryotic systems (Kim *et al*., 1995). Gel anomaly experimemts have concluded that the macroscopic magnitude of DNA bending is approximately 17 to 21° per A-tract (Koo *et al*., 1990), and in the direction of the minor groove at the center of the A-tract stretches (Zinkel & Crothers, 1987).

The structural effect of A-tracts in DNA at the molecular level and the role of A tracts in DNA-bending phenomena is not a settled issue (Lavigne *et al*., 1997; Olson & Zhurkin, 1996; Sundaralingam & Sekharudu, 1988). The various models describing how DNA bending might relate to A-tracts can be generally categorized as ''bent A-tract'' or ''straight A-tract'' models. In the AA wedge model, an example of the former category advanced by Trifonov and co-workers (Trifonov, 1980), each ApA step in a tract is bent by a small ''wedge angle''. Each ApA wedge is comprised of a combination of base-pair roll and tilt, whereas random-sequence DNA is straight, or at least averages to straight. Much of the current data on DNA bending in solution observed in gels or cyclization experiments has been successfully interpreted by a refined example of an AA wedge model, the model developed *via* regression analysis (Bolshoy *et al*., 1991). Despite its successes, there are subsequent indications that the reported fit is not unique (Y. Liu & D.L.B. unpublished results). Analysis of the results of solution studies of A-tracts is complicated by the fact that the properties of A-tracts in solution have been observed to exhibit noted dependencies on both temperature and salt conditions (Diekmann, 1989). A-tract DNA is also reported to undergo ''premelting'' structural transitions, possibly involving bending, at close to physiological conditions (Chan *et al*., 1993).

One form of a straight A tract model is the junction model, which holds that A-tracts and random-sequence DNA are both essentially straight, and that bending occurs at the junction of these two forms. A specific form of junction model was initially proposed by Crothers and co-workers (Koo & Crothers, 1988). Oligonucleotide crystal structures (Berman *et al*., 1992) provides extensive data consistent with ''straight A-tracts'' and can be viewed as being consistent with a junction model of DNA bending (Young *et al*., 1995). The details of the junction bending observed in crystal structures of A-tract sequences are slightly different from those proposed in the Crothers model. However, crystal structures are available only on relatively short oligonucleotides, and are subject to packing effects that may (DiGabriele *et al*., 1989; Narayana *et al*., 1991) or may not (Dickerson *et al*., 1987, 1991) influence the results.

Subsequent variations on the idea of straight A-tract models have been proposed (Goodsell &

Dickerson, 1994), particularly the bent general sequence model (Olson *et al*., 1993), which postulates that bending occurs not just at junctions but more generally throughout the non-A-regions of a sequence. The evidence for this is primarily crystallographic, and for the reasons noted above, is significant but not totally unequivocal. Adding to the confusion is the recent reports that ApA steps in crystals may be sensitive to the effects of organic solvents such as methylpentane diol (MPD), a common co-crystalizing agent in the preparation of samples for X-ray diffraction studies (Sprous *et al*., 1995). However, the nature of this effect is disputed (Dickerson *et al*., 1996), and an explanation as to why this should preferentially effect ApA steps and not steps involving other nucleotides has not yet been successfully advanced.

The study of the effects of hydroxyl radical cleavage on sequences with phased A-tracts has revealed evidence for anomalous changes within A-tracts and a progressive change moving 5′ to 3′ within the A-tracts of a sequence. The interpretation of this result advanced by Tullius and Burkhoff (Burkhoff & Tullius, 1987; Tullius & Burkhoff, 1988) was one of a progressive narrowing of the minor groove, but any change that might affect access of the OH radical to sugar or backbone protons in the minor groove could, in principle, account for the results. A particular question of interest is thus the extent to which the hydroxyl radical cleavage results may be evidence for a wedge model of bending. Footprinting experiments support the idea that the addition of MPD converts the behavior of A-tract from anomalous to ''normal'' (Ganunis *et al*., 1996).

Molecular dynamics (MD) computer simulation has been used recently to study DNA bending in several short oligonucleotide sequences in solution, and provides an independent theoretical means of investigating further the problems identified above (Beveridge *et al*., 1998). MD can, in principle, provide a complete theoretical description of DNA structure and motions including solvent water and counterions, and with the advent of supercomputers is becoming a valuable independent means of developing models and interpreting diverse experimental data on DNA structure in solution (Beveridge & Ravishanker, 1994). However, while MD is a well-defined theoretical methodology, approximations in the underlying force-field, the sensitivity of results to simulation protocols and the practical limit of MD simulations to the picosecond time-scale have been the source of limitations in the development of accurate dynamical models of DNA.

Recent advances in computer power and simulation methodology have enabled the use of MD methods to simulate DNA, including solvent water and mobile counter-ions and co-ions for trajectories extended well into the nanosecond region of time. A new version of the AMBER force-field, proposed by Cornell *et al*. (1995), including specific improvements in nucleic acid parameters and designed for use with full solvent has been incorporated in the AMBER suite of programs, release 4.1 (Pearlman *et al*., 1995). In addition, a treatment of long-range electrostatic interaction potentials, the particle mesh Ewald (PME) method (Darden *et al*., 1995; York *et al*., 1994), has been proposed to deal with the long-standing issue of the treatment of truncation effects in MD protocols. Independent studies using AMBER 4.1 have demonstrated thus far that the Cornell *et al*. (1995) force-field, used with PME, supports an accurate model of *B*-form DNA in solution (Cheatham *et al*., 1995; Duan *et al*., 1997; Young *et al*., 1997a, 1997b). and have provided a basis for studies of the *A* to *B* transition in solution (Cheatham & Kollman, 1996; Cheatham *et al*., 1997; B. Jayaram, D. Sprous, M.A.Y. & D.L.B., unpublished results), the propensity of a *B/A/B* structure implicated in protein binding to be assumed intrinsically by the TATA box binding sequence (Flatters *et al*., 1997), DNA/RNA hybrid structures (Cheatham & Kollman, 1997) and novel RNA structures (Miller & Kollman, 1997).

Here, we describe a theoretical model of a DNA oligonucleotide duplex featuring A-tracts phased by a full helix turn based on MD. We consider the extent to which this model agrees with and accounts for relevant experimental data on axis bending. Finally, we investigate the relationship of A-tract sequences to DNA bending and other aspects of DNA helix morphology.

Results

The results from the MD simulations performed in this study are summarized in Table 1. The Curves algorithm (Lavery & Sklenar, 1989, 1996) was used to obtain values for the curvilinear path-length *L* and end-to-end distance *R*, assuming that oligonucleotide end effects and fraying are minimal. Here, we describe curvature in terms of both the percentage reduction in helix path-length *L/R* (shortening), and the angle between local helical axis vectors of terminal base-pair steps (angle). Two sets of these values are reported in Table 1. The values on the left are calculated from a single average structure constructed from the average Cartesian coordinates for all atoms over the length of each MD trajectory. The values on the right are the ensemble averages values, or the average value for each parameter when calculated independently for structures sampled every 5 ps over each trajectory. Hagerman (1990) and others (Prevost *et al*., 1993; Schellman & Harvey, 1995) have proposed a variety of methods for estimating the persistence lengths of an oligonucleotide sequence given information about the structure, but the methods are not uniquely defined, and *L/R* and angle indices are sufficient for the purposes of this study.

The phased A-tract trajectory including $MgCl_2$ (simulation (c)) was extended to 5 ns, and we provide here more details on this particular run and examine the results to ascertain the model of bend-

Table 1. Average bend angles and helix shortening

Sequence	Salt	Simulation length (ps)	Shortening ave str (%)	Angle ave str (deg.)	Shortening ens ave (%)	Angle ens. ave (deg.)
A-tract (a) (ATAGGCAAAAAATAGGCAAAAATGG)	min. Na^+	5000	0.4	14.7	3.7	25.9
A-tract (b) (ATAGGCAAAAAATAGGCAAAAATGG)	K^+, Cl^-	5000	1.3	27.0	4.0	29.9
A-tract (c) (ATAGGCAAAAAATAGGCAAAAATGG)	K^+, Cl^-, Mg^{2+}	5000	1.4	30.0	4.2	30.8
*Bam*HI (CGGGATCCCGCGGGA-TCCCGCGGGATCCCG)	K^+, Cl^-, Mg^{2+}	5000	1.2	17.8	4.9	29.9
EcoRI (GCGAATTCGCGCGAA-TTCGCGCGAATTCGC)	Na^+, Cl^-	3000	0.7	19.0	0.7	19.0

All simulations were initiated from a canonical *B*-DNA starting structure, were solvated to approximately 14 Å beyond the DNA in all directions, and were simulated under nPT conditions. Simulation solvent included the following concentrations of the indicated ionic species: 60 mM NaCl, 60 mM KCl, 10 mM $MgCl_2$, plus DNA-neutralizing cations in a ratio equal to their partial molar equivalents in the added salt (ie. all Na^+, all K^+, or 6:1 K^+ to Mg^{2+}). Ion concentrations are calculated based upon the volume of the simulation cell. Further details are included in Methods.

Average structure (ave str) values are calculated from a single structure computed from the average atomic positions over the entire MD trajectory. Ensemble average (ens ave) values are the values of each parameter averaged over values of individual snapshots calculated every 5.0 ps over the MD trajectory.

ing supported by the MD. The structural rms exhibits an oscillatory behavior about the time-averaged structure with magnitudes of approximately 1 to 1.5 Å and rests at about 7 Å rmsd from the canonical *B*-form structure, which served as the starting conformation for the trajectory. The *Bam*HI

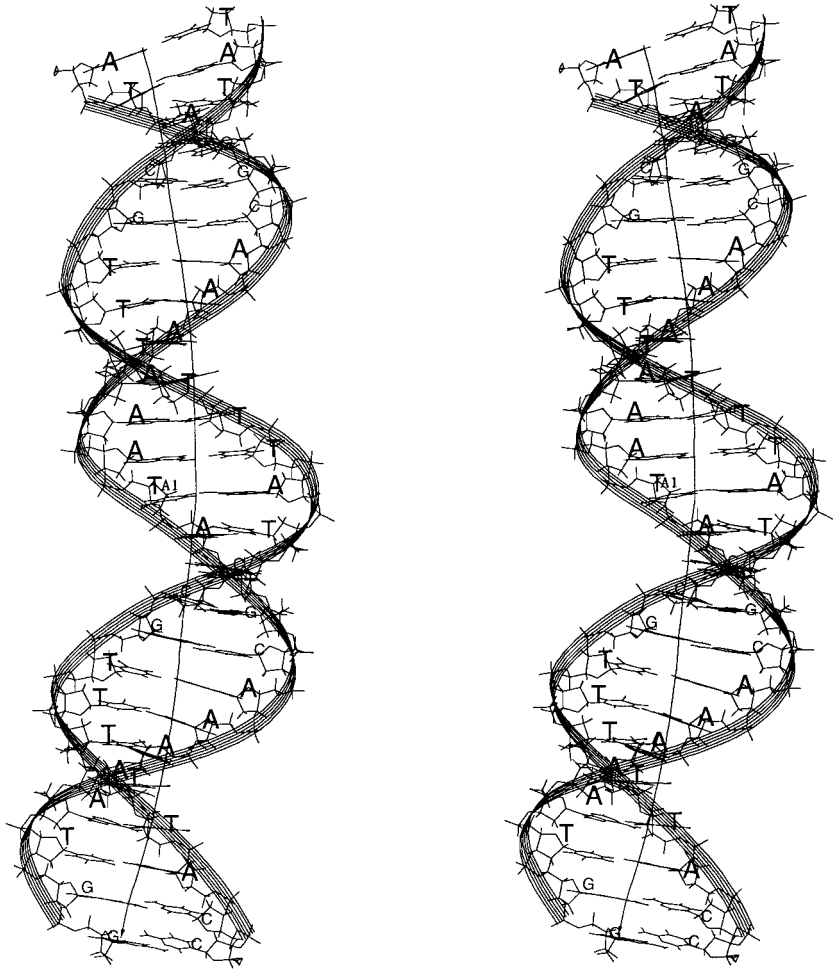

Figure 1. The 5.0 ns MD average structure for the phased A-tract sequence d(ATAGGCAAAAAA-TAGGCAAAAATGG), simulated in 10 mM $MgCl_2$, 60 mM KCl saline solution.

control sequence, which was simulated in the same ionic conditions as (c), also showed reasonable stability and arrived at about 5.8 Å rms from the canonical *B*-form after approximately 1 ns of MD. The full trajectory of the control was also extended to 5 ns. The initial drift to the observed 6 to 7 Å rms over the initial ~300 to 500 ps of the simulations defines the equilibration step. The 1 to 1.5 Å variations in rms about the calculated average structure are thermal fluctuations.

Our results indicate that the average MD structure for the phased A-tract sequence at salt conditions of (c) above, shown in Figure 1, exhibits bending behavior consistent with the experimental results obtained on this sequence at similar ionic concentrations (Crothers *et al.*, 1992; Gartenberg & Crothers, 1991). The calculated bending per A-tract is 15.4°, which compares quite favorably with the experimentally measured value of 17-21° determined from cyclization kinetics (Crothers *et al.*, 1992). As shown in the time-series of the bending behavior in Figure 3, transient fluctuations of the overall helical curvature approaching 90° were observed at multiple points during the trajectory. Thus, under appropriate environmental conditions, the curvature of the MD model of the 25 bp phased A-tract sequence is in close correspondence with the observed behavior, and at the same time provides atomic level detail of the underlying molecular structures.

The average MD structure for the corresponding *Bam*HI control is shown in Figure 2. The overall bend angle calculated for the MD average structure of the *Bam*HI 30 mer is 17.8°. Looking at the average conformations of each sequence, the *Bam*HI control sequence is considerably less bent than the slightly shorter phased A-tract sequence, but the helical axis of the control sequence is by no means perfectly straight. The observation that the average conformation for the *Bam*HI sequence demonstrates considerable overall curvature prompts us to describe the nature of the bending in the two cases in more detail. The analysis provided in Figure 4(a) utilizes a polar plot to display both the magnitude of global helical bend and the angular direction of that bend. The magnitude of the helix bend is plotted as the radial coordinate and the direction of bending is displayed within the reference frame of the central step of each sequence. In this convention, bending towards the direction of the major groove (MG) at the central step of the helix is plotted in the northern hemisphere of the plot, and bending in the direction of the minor groove at this step is plotted in the southern hemi-

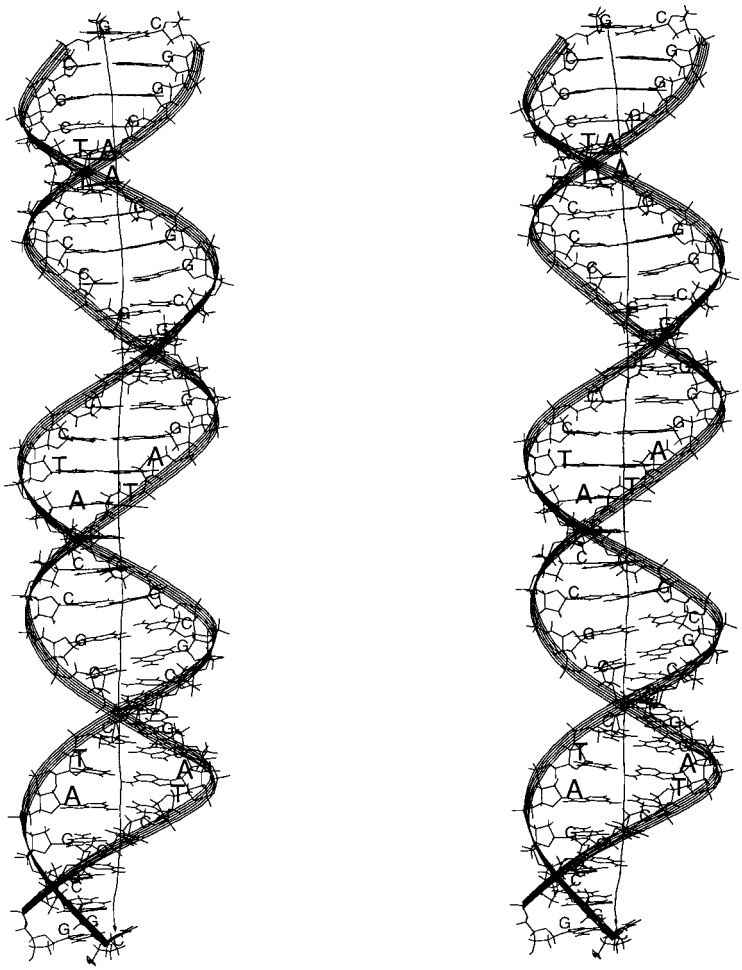

Figure 2. The 5.0 ns MD average structure for the control sequence d(CGGGATCCCGCGGGATCCCG-CGGGATCCCG), simulated in the same saline environment as reported for Figure 1.

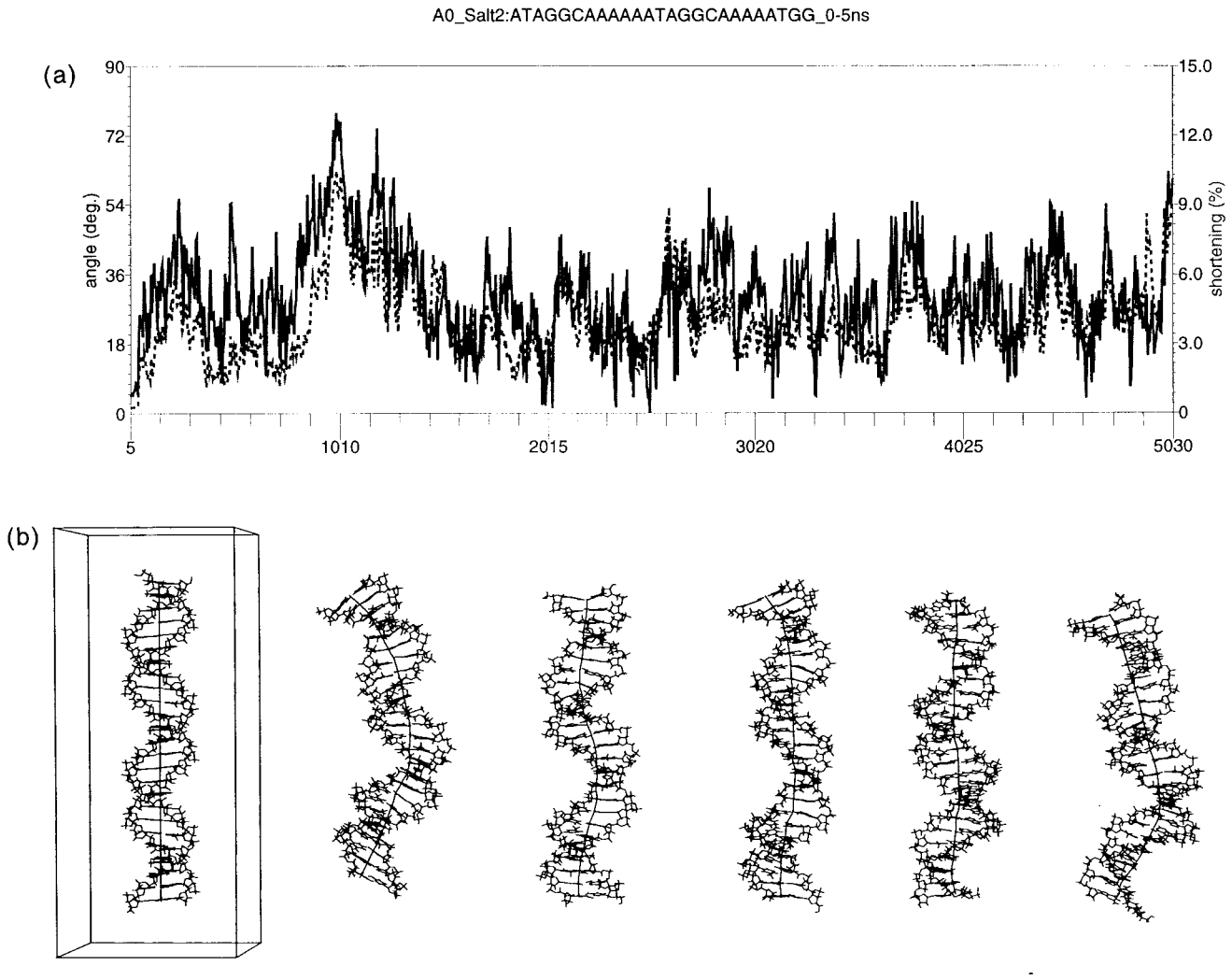

Figure 3. Plot of the time evolution of axis bending in the A-tract sequence, with representative snapshots spaced approximately 1ns along the trajectory. Quantification of the direction of bending has been done by the Curves program (Lavery & Sklenar, 1996), which reports the direction of the angle formed between the helical axis vectors for the first and last base-pairs of the sequence (contnuous line), as well as the percentage shortening of the helix end-to-end distance/curvilinear path length (broken line). The solvent molecules have been removed from the structures for clarity of presentation.

sphere. Individual points are for structures separated by 10 ps throughout the course of the trajectory, and viewed together comprise a probability density. The results indicate that the direction of bending in the phased A-tract sequence is in a generally unchanging direction over time, whereas the direction of bending for the control sequence is highly variable. The plots in Figure 4(b) show the identical bending analysis displayed within the reference frame of the 2 bp steps located at the center of each of the two A-tracts in the phased A-tract sequence. The results show that the overall helix bending is concerted, and towards the minor groove with respect to the centers of both of the A-tracts. The phased A-tracts thus promote a constructive effect in the bending, which organizes the overall bending in a direction that is fairly unchanging throughout the trajectory, a quality not exhibited in the control.

The bent A-tract model emerging from the MD calculations contains a strong dynamic component, which is evidenced by the following two observations. First, the largest difference in bending angle observed in the phased A-tract DNA and the control DNA is seen in a time-averaged sense rather than in individual snapshots. This is due to the constant bending direction observed in the A-tract sequence, compared with the changing bend direction found in the control. The bending direction in the latter case tends to cancel or average itself out when averaged over time. The manifestation of this difference is visible in the much stronger correlation between the values of the bending angle in the average structure and the ensemble averaged values for the A-tract sequence as compared with in the control. As shown in Table 1, the average structure values and average ensemble values are 30.0° and 30.8°, respectively, for the

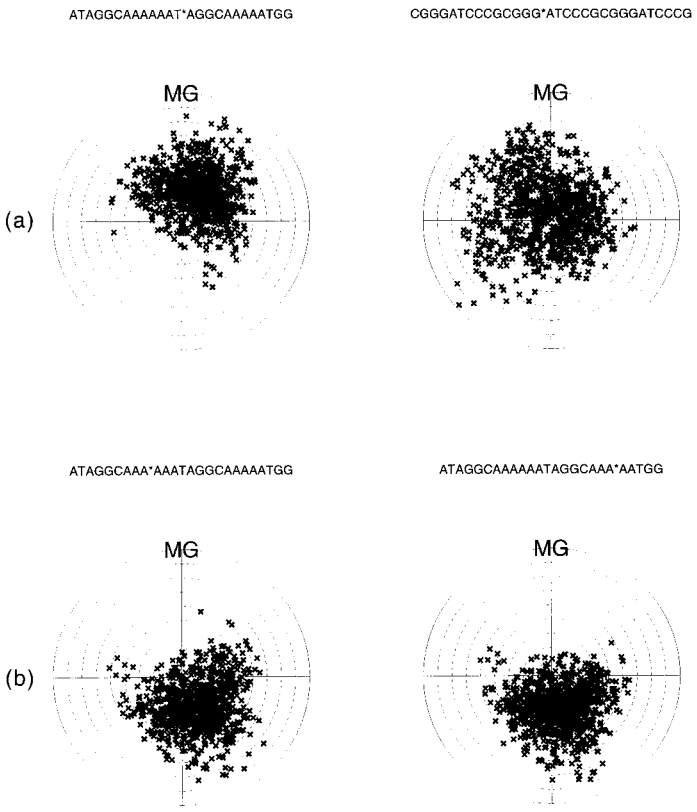

Figure 4. Plot of the overall helix bending direction and magnitude for (a) the A-tract simulation and (b) the *Bam*HI simulation. The bend direction was computed with Curves (Lavery & Sklenar, 1996) via the angle between the top and bottom base-pair perpendicular vectors. The bending direction is presented in the reference frame of the central base-pair step of each sequence, with bending towards the major groove (MG) plotted in the northern direction and bending towards the minor groove plotted in the southern direction. (c) An alternative plot of the overall helix bending magnitude and direction for the A-tract simulation. The bending is plotted in the reference frame of the two steps at the center of each of the A-tracts (indicated with an asterisk). This presentation illustrates the unchanging directionality of the overall bend, in a concerted direction compressing the minor groove (south on the plots) at the center of both A-tracts.

phased A-tract sequence, and 17.8° and 29.9°, respectively, for the control sequence. The second dynamic component of the model lies in the fluctuating nature of the bend magnitude. Figure 3 illustrates how the phased A-tract sequence reaches a bend maximum at two distinct times during the trajectory, exhibiting anharmonic fluctuation. Both of these dynamic properties of the model could have important implications in understanding cellular processes involving DNA in a sequence-specific manner.

The helicoidal parameters X-displacement (*XDP*) and inclination (*INC*) and the sugar conformations *P* of the nucleic acid backbone are structural indices that distinguish *B*-form from *A*-form in a right-handed DNA double helix (Ravishanker *et al.*, 1989). For canonical *B*-form DNA, $XDP = 0$ Å, $INC = 0°$ and $P = 154°$, i.e. C2′-*endo* sugar pucker. For *A*-form DNA, $XDP = -5.2$ Å, $INC = 20°$ and $P = 14°$, i.e. C3′-*endo* sugar pucker. Averaged over the production portion of the 5 ns trajectory, the phased A-tract sequence shows $XDP = -2.63$ Å and $INC = 2.92°$, with sugar puckers mainly in the C2′-*endo*/O1′-*exo* region (~140°). The control sequence shows $XDP = -2.48°$, $INC = 4.02°$, and similar close-to C2′-*endo* sugars. The results indicate that both structures remain closer to the *B*-form values over the entire course of each simulation, indicating that the dynamical structure of the MD model of each sequence is clearly in the *B* family, although the helicoidal analysis shows a distinctly negative *XDP*, intermediate between values found in canonical *B* and *A* forms of DNA.

Average values for the helicoidal parameters *ROL* (roll) and *TLT* (tilt) as a function of base-pair step for the phased A-tract sequence are shown in Figure 5. The results indicate the presence of a small but constant amount of slightly positive *ROL* angles within the A-tracts, as compared with much larger deviations from zero magnitudes, mostly on the positive side, in the flanking sequences. The *TLT* parameter shows small magnitude negative values within the A-tracts, and small magnitude positive values in the non-AA steps. Thus, the bending model that emerges from the MD is comprised of relatively but not perfectly straight A-tracts, with large axis deflections at the A-tract junctions and within the non A-tract stretches. At the base-pair step level, the principle origin of the macroscopic bending is towards the major groove of the helix (positive *ROL*) in non-A tract regions of the sequence.

The average *ROL* and *TLT* values for each step in the sequence as calculated from *B*-form structures found in the Nucleotide Data Bank (Young *et al.*, 1995), determined from X-ray crystallography, are indicated in Figure 5 as a thin continuous line. The small degree of bending within A-tracts is a characteristic similar to that observed for A-tract sequences in the 15 examples of A-tract sequences in the crystallographic data base. Unlike the bending observed in the AA step, however, many of the non-AA steps deviate considerably from the currently available crystallographic representations of each of these steps. This discrepancy of the bending angles observed at the base-step level may be

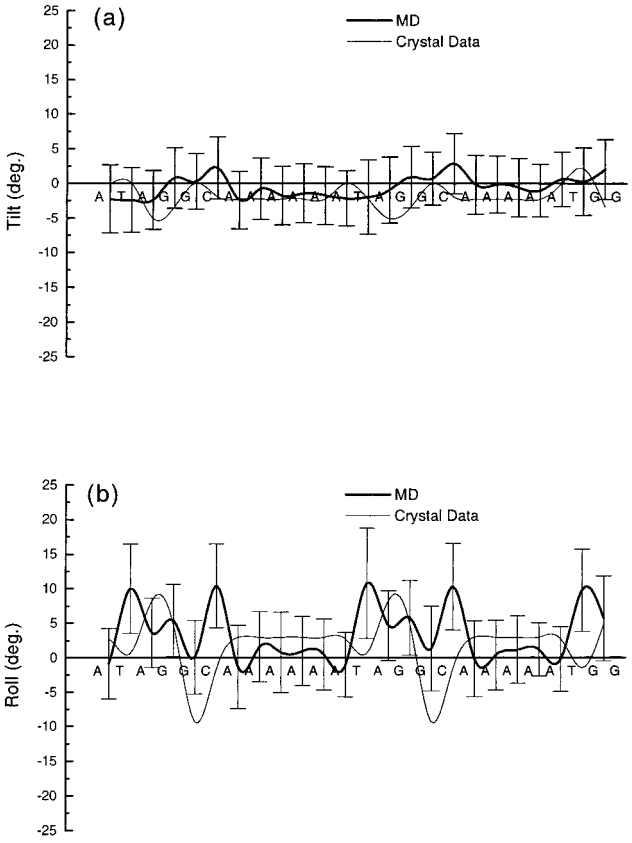

Figure 5. Tilt and Roll values from the A-tract sequence. Values plotted as the thick line are the ensemble average ±s.d. of fluctuation from MD simulation (c). Corresponding average *Tilt* and *Roll* values for the *B*-form DNA crystal structures; examples of each step (from Young *et al.*, 1995) are plotted as thin lines.

the result of neglecting sequence context effects and related base-step level bendabilities in the analysis of the crystallographic data. This result may thus reflect on the inability of a dinucleotide model to adequately predict DNA curvature in all cases. It is possible that the bending observed in a CA step is different when the CA step is located at the 5′ end of an A-tract compared with a CA step located in another context.

Footprinting experiments on oligonucleotides indicate that A-tracts are well differentiated from random sequence DNA in diverse systems, and show evidence of a progressive change occurring 5′ to 3′ within the A-tracts. Interpretation of the data in terms of minor groove narrowing has been advanced (Tullius & Burkhoff, 1988). In the present study, the minor groove widths of the MD models of d(ATAGGCAAAAAATAGGCAAAAATGG) and d(CGGGATCCCGCGGGATCCCGCGGGATCCCG) have been computed using the spline-fitting algorithm in Curves (Lavery & Sklenar, 1989, 1996; Stofer & Lavery, 1994), and are displayed at each point along the helix in Figure 6. The analysis of the MD model of d(ATAGGCAAAAAATAGG-CAAAAATGG), presented in Figure 6(a), shows that the structure exhibits a distinct narrowing of the minor groove in the A-tract regions, and a progressive narrowing of the minor groove region of the A-tracts occurring 5′ to 3′ in the sequence. The corresponding results for the control sequence, Figure 6(b), show no evidence of this effect. In addition to the observed A-tract narrowing, a highly conserved property of this sequence, as well as other A-tract sequences we have studied (data not shown), is the considerable widening of the minor groove at the 5′ end of the A-tracts, a novel observation that is consistent with the reported footprinting data. Thus the MD model provides, with no prior assumption or aims to reproduce this effect, an independent confirmation of the interpretation of the footprinting data on diverse phased A-tract sequences advanced by Tullius and co-workers (Tullius & Burkhoff, 1988). Despite the observed progressive 5′ to 3′ narrowing of the minor groove, our analysis has not found any indication of any other progressive 5′ to 3′ changes occurring within A-tracts in the MD model that could be consistent with a wedge model of A-tract bending.

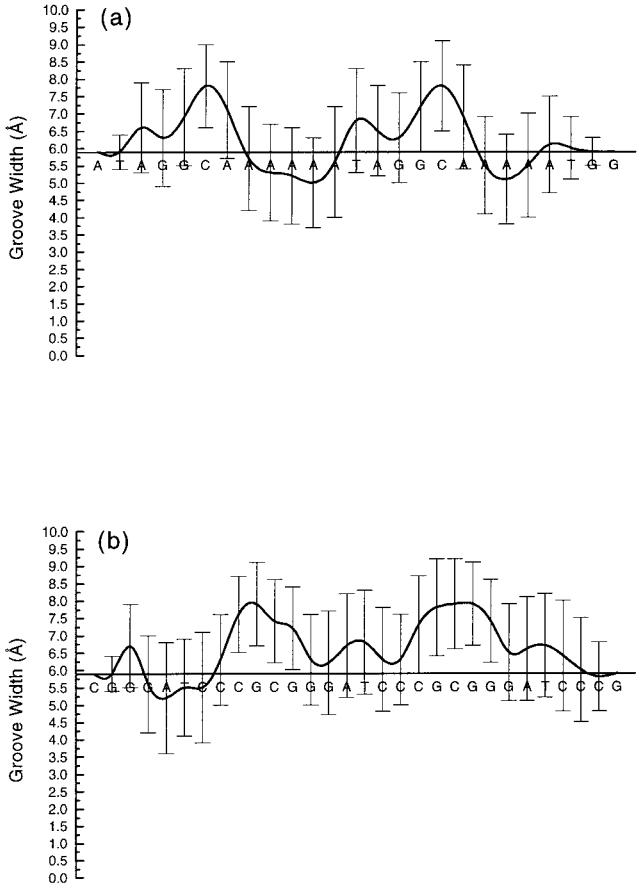

Figure 6. Minor groove widths calculated with Curves (Lavery & Sklenar, 1996; Stofer & Lavery, 1994) for (a) phased A-tract sequence, (b) control sequence. Vertical bars indicate 1 s.d. The corresponding value of the minor groove width for canonical *B*-form DNA is 5.89 Å (indicated by the position of the *x*-axis).

The effects of different salt conditions on the measured curvature of the phased A-tract sequence are illustrated in Table 1. The statistical measures of curvature show that overall curvature increases significantly upon changing the buffer from neutralizing Na^+ (simulation (a)) to conditions of 60 mM added KCl (simulation (b)). This result is consistent with an experimental report that the addition of Na^+ to A-tract gel retardation experiments can reduce measured anomaly (Diekmann & Wang, 1985). The curvature increases slightly upon the addition of divalent Mg^{2+} to the KCl system (simulation (c)), also consistent with experiment (Diekmann, 1987; Hagerman, 1984). While the Mg^{2+} effect is small, it is probable that the measurable affect of Mg^{2+} would be amplified in sequences with increased numbers of A-tracts. The magnesium ions interact with the DNA in a fully hydrated state, consistent with experiment (Buckin *et al*., 1989, 1994; Fujimoto *et al*., 1994).

The magnesium ions interact with sites along the phosphate backbone, the major groove, and the minor groove in a non-uniform and sequence-dependent manner. A representation of the statistical Mg^{2+} ''local reference frame'' ion distribution around the DNA, computed over the 5ns trajectory, is shown in Figure 7. The local reference frame distribution probability shown is calculated by initially calculating and recording an ion-DNA g(R), partitioning the ions using an atom-based proximity criterion (Mehrotra & Beveridge, 1980; Mezei & Beveridge, 1986), over the entire length of the trajectory. The atom-based g(R) values are then mapped onto a 0.5 $Å^3$ 3D grid surrounding the average DNA conformation in order to generate the image presented in Figure 7. The localization of divalent cations we observe at the 5′ end of both A-tract minor groove regions we see has been observed *via* NMR with Mn^{2+} in another A-tract sequence (Hud & Feigon, 1997). Mg^{2+} and K^+ are also observed to interact with sites in the major groove of the A-tract flanking sequences, and are often found on the concave surface of a positive *ROL* bend. Average residence times of the mobile ions with individual DNA atoms are indicated in Figure 7 and range from just a few picoseconds to approximately 100 ps. The residence times were calculated using a procedure adopted from Impey *et al*. (1983). Sites with the longest residence times with Mg^{2+}, such as the backbone phosphate oxy-

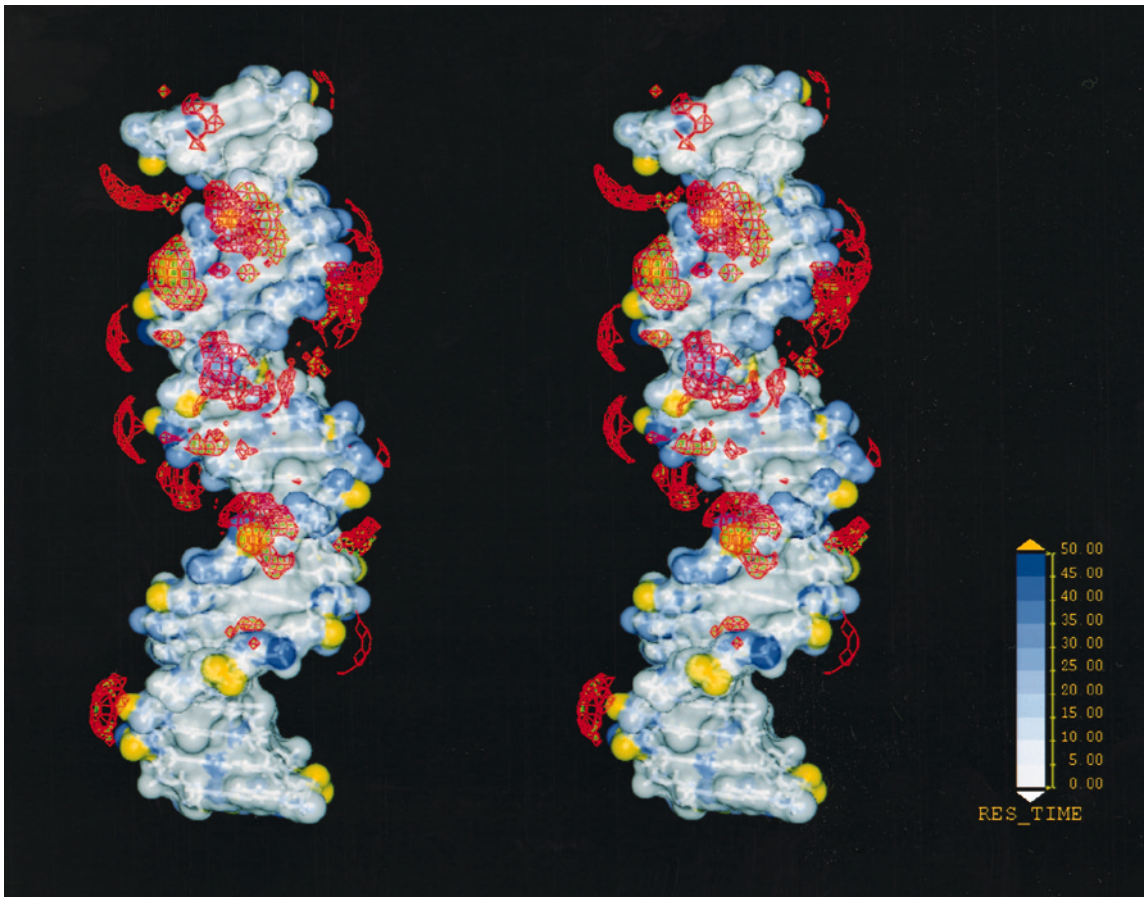

Figure 7. Local reference frame probability distribution and residence times of Mg^{2+} interactions with the phased A-tract DNA sequence (simulation (c)). Two mesh iso-concentration contours are plotted: 10× bulk (green) and 5× bulk (red). The solvent-accessible surface of the stereo image pair is colored to indicated the average residence time of Mg^{2+} with each atom. Interaction times are colored according to the scale on the right (in ps). All DNA-Mg^{2+} interactions are mediated by at least one water molecule.

gen atoms, do not necessarily correlate with the sites of highest ion probability.

Summary and Conclusions

Molecular dynamics simulations based on the AMBER 4.1 force-field were used to generate dynamical models for DNA oligonucleotide sequences of greater than two full helical turns in saline solution. One sequence has two A-tracts spaced by a full turn of a *B*-form double helix, and others, which serve as controls, do not. Our results indicate that at experimental salt conditions, and in particular in the presence of divalent cations, the MD model exhibits the full effect of phased A-tracts on DNA bending. Thus, with no disposable parameter applied specifically to DNA bending, the MD model of d(ATAGGCAAAAAATAGGCAAAAATGG) gives an independent account of the observed behavior of phased A-tracts in nucleosomes, gel experiments and cyclization kinetics in terms of intermolecular forces and motions, and behaves in a manner predicted from independent prior interpretations of footprinting experiments.

The characteristics of the MD model resulting from the simulation are as follows: (a) the overall bending of the phased A-tract sequence is ca 15° per A-tract, as compared with 17 to 2° inferred from experiment; (b) the control sequence, lacking phased A-tracts, is instantaneously bent, but the changing directionality of the bend causes the time-averaged conformation to be much straighter; (c) the bending magnitude increases as a function of added salt, and the magnitude increases in the presence of the divalent ion Mg^{2+}; (d) ions are coordinated with individual DNA atoms for periods approaching 100 ps and magnesium ions are observed to be localized, in a hydrated form, around sites on the DNA with sites in both grooves for periods exceeding 1 to 2 ns; (e) the phased A-tract bending is oscillatory with a period of at least 3 to 4 ns, and the period of oscillation is decreased by the presence of salt; (f) transient dynamical fluctuations reaching bends as strong as 45° per A-tract are observed during the dynamics; (g) the overall bending of a sequence with phased A-tract can be concerted in time, and thus amplified by phasing with respect to the *B*-form DNA helical repeat of approximately 11 bp per turn; (h) the individual AA steps in the A-tracts are close to straight, as observed in oligonucleotide crystal structures, showing only a slight but consistent bend towards the minor groove; (i) the bending in the phased A-tract sequence is located in the non-A-tract regions of the sequence, particularly at the junctions of A-tracts with the flanking sequences, but also to some extent within the random sequence region; (j) the analysis shows the bending to occur *via* a positive base-pair roll in the non-AA steps of the sequence; (k) the minor groove of the A-tract is wide relative to that of canonical *B*-DNA at the 5′ end of the A-tract, and narrows progressively towards the 3′ end, in agreement with footprinting data.

The results we have obtained describe the properties of A-tract DNA in a solution environment and the structural properties we have reported represent intrinsic properties at 298 K. The sequence-dependent deformability of DNA is another biologically relevant intrinsic DNA property, and features of A-tract DNA listed above may also be predictive of intrinsic inducible properties of A-tracts as well. In particular, the results shown in Figure 4(b) indicate that there is a considerable energetic difference between bending in the direction of the minor groove at the A-tract center compared with bending into the major groove. This suggests that it is energetically unfavorable to curve A-tract DNA such that it bends in the direction compressing the major groove at its center, because this type of curvature was never observed during the A-tract DNA simulations.

For DNA sequences with A-tracts phased with respect to a full turn of the *B*-form helix, MD simulations support what is effectively a junction model of bending with an admixture of mixed sequence model. This result is derived from an MD model that is independently validated by a series of recent successes in describing nucleic acid structure and motions (Cheatham *et al.*, 1995; Young *et al.*, 1997a,b).

Methods

A series of four isothermal-isobaric (T,P,N) ensemble MD simulations were performed on the oligonucleotide duplex d(ATAGGCAAAAAATAGGCAAAAATGG) in water, each configured with different species, concentrations, and/or starting positions of the elemental ions: Na^+, K^+, Mg^{2+} and Cl^-. In each case, a net neutral charge on the system is maintained. The conditions simulated include: (a) no added salt, neutralizing Na^+ cations, (b) 60 mM KCl, 10 mM $MgCl_2$ added salt, plus neutralizing cations (K^+, Mg^{2+} in an equal ratio as in the added salt), with the ions positioned *via* an *in vacuo* Monte Carlo algorithm; (c) same conditions as (b), but with random initial ion positioning (maintaining a minimum 6 Å clearance); and (d) 60 mM KCl added salt, plus neutralizing cations (K^+). In all other matters, the simulations were configured as similar to each other as possible, although run lengths of course vary according to the observed characteristics of each trajectory with respect to stability (see below and Discussion). The control sequence d(CGGGATCCCGCGGGATCCCGCGGGATCCCG) was simulated under conditions identical with (c) above. The calculations employed the all-atom force-field described by Cornell *et al.* (1995), the TIP3P model for water (Jorgensen, 1981) and were carried out using the suite of programs AMBER 4.1 (Pearlman *et al.*, 1995). The van der Waals parameters for the magnesium ions were parameterized by adapting values from Aqvist (1990), which accurately reproduce the hydration energy of Mg^{2+} in a similar water model (SPC). Starting DNA configurations for each case were the canonical forms of the *B*-DNA double helix (Arnott *et al.*, 1976).

Following placement of the counterions about a canonical *B*-form of the DNA structure, each system was configured into a rectangular prism and hydrated by TIP3P water molecules in a pre-equilibrated configuration. The box dimensions were truncated to achieve a minimum distance of approximately 14 Å beyond all DNA atoms in all directions, resulting in a box size of approximately 46 Å × 46 × 110 Å for the 25-mer, solvating the DNA with approximately 6500 water molecules in each case. The effective concentration of the DNA sample within the periodic box is approximately 10 mM (calculated by volume). Prior to MD, the various starting configurations were subjected to a series of energy minimizations to relieve any local atomic clashes. All PME calculations were carried out with a 9 Å cutoff for direct space nonbonded calculations and a 0.00001 Ewald convergence tolerance for the long-range electrostatic interactions.

Each MD was initiated with several rounds of semi-restrained and eventually unrestrained minimizations of the entire system followed by heating, equilibration and unrestrained. (T,P,N) ensemble MD. Harmonic restraints of 25 kcal/mol $Å^2$ were placed on DNA and ion atom positions during the first round of 500 steps of minimization. The restraints were relaxed on the ions more quickly than on the DNA atoms over the course of five subsequent 100-step minimizations. The final round of 500 steps of minimization involved all atoms of the systems. Heating and initial system equilibration was performed in a parallel semi-restrained fashion as follows. First, 10 ps of heating was performed on the constant volume system while restraining the DNA and ion atom locations. This was followed by reducing the restraints on the ions more quickly than on the DNA atoms up to 25 ps. Unrestrained constant volume dynamics were continued for another 5 ps, at which time constant temperature, constant pressure MD (isothermal-isobaric ensemble) was initiated, utilizing the Berendsen algorithm for temperature bath coupling (Berendsen *et al.*, 1984) and a 2 fs time-step. The system energy was stable when coupled with a SHAKE constraint of 0.00001 Å on all covalent bonds involving hydrogen atoms. To maintain the alignment of the DNA within the center of the rectangular box, the Sander module of AMBER 4.1 was modified to remove translations and rotations of the solute center of mass at every 100 steps of MD. The center of mass energy removed by this procedure was replaced by appropriately scaling the resulting solute atom velocities to conserve kinetic energy. The MD simulations were performed on the Cray C90 and the T3D parallel computer at the Pittsburgh Supercomputer Center, the SGI power challenge array and Origin2000 array at NCSA, and locally at Wesleyan on SGI workstations.

Acknowledgments

This research was supported primarily by grant #GM-37909 from the National Institutes of Health. M.A.Y. is the recipient of an NIGMS Traineeship in Molecular Biophysics, from grant # GM-08271 to Wesleyan University. Computer graphics analyses were facilitated by a grant from the Dreyfus Foundation and use of the computer programs MD ToolChest (Ravishanker, 1991), UCSF Midas-Plus (Ferrin *et al.*, 1988; Huang *et al.*, 1991), and InsightII (Biosym/MSI, 1995). Computer time was provided for these projects by the Pittsburgh Supercomputer Center, the Frederick Biomedical Supercomputer Center of the National Cancer Institute, NIH, and the National Center for Supercomputer Applications, Illinois. The authors gratefully acknowledge discussions and advice on this project from Dr G. Ravishanker and Dr Richard Lavery.

References

Aqvist, J. (1990). Ion-water interaction potentials derived from free energy perturbation simulations. *J. Phys. Chem.* **94**, 8021–8024.

Arnott, S., Campbell-Smith, P. J. & Chandrasekaran, R. (1976). Atomic coordinates and molecular conformations for DNA-DNA, RNA-RNA, and DNA-RNA helices. In *CRC Handbook of Biochemistry and Molecular Biology* (Fasman, G., ed.), vol. 2, pp. 411–422, CRC Press, Cleveland.

Berendsen, H. J. C., Postma, J. P. M., van Gunsteren, W. F. & DiNola, A. (1984). Molecular dynamics with coupling to an external bath. *J. Chem. Phys.* **81**, 3684–3690.

Berman, H. M., Olson, W. K., Beveridge, D. L., Westbrook, J., Gelbin, A., Demeny, T., Hsieh, S.-H., Srinivasan, A. R. & Schneider, B. (1992). The nucleic acid database: a comprehensive relational database of three-dimensional structures of nucleic acids. *Biophys. J.* **63**, 751–759.

Beveridge, D. L. & Ravishanker, G. (1994). Molecular dynamics studies of DNA. *Curr. Opin. Struct. Biol.* **4**, 246–255.

Beveridge, D. L., Young, M. A. & Sprous, D. (1998). Modeling of DNA via molecular dynamics simulation: structure, bending, and conformational transitions. In *Molecular Modeling of Nucleic Acids* (Leontis, N. B. & Santa, Lucia J. J., eds), vol. 1, pp. 260–284, American Chemical Society, Washington, DC.

Biosym/MSI (1995). InsightII, edit 95.0, Biosym/MSI, San Diego.

Bolshoy, A., McNamara, P., Harrington, R. E. & Trifonov, E. N. (1991). Curved DNA without A-A: experimental estimation of all 16 DNA wedge angles. *Proc. Natl Acad. Sci. USA*, **88**, 2312–2316.

Bracco, L., Kotlarz, D., Kolb, A., Diekmann, S. & Buc, H. (1989). Synthetic curved DNA sequences can act as transcriptional activators in *Escherichia coli*. *EMBO J.* **8**, 4289–4296.

Buckin, V. A., Kankiya, B. I., Sarvazyan, A. P. & Uedaira, H. (1989). Acoustical investigation of poly(dA)poly(dT), poly[d(A-T)], poly(A)poly(U) and DNA hydration in dilute aqueous solutions. *Nucl. Acids Res.* **17**, 4189–4203.

Buckin, V. A., Kankiya, B. I., Rentzeperis, D. & Marky, L. A. (1994). Mg^{2+} Recognizes the sequence of DNA through its hydration shell. *J. Am. Chem. Soc.* **116**, 9423–9429.

Burkhoff, A. M. & Tullius, T. D. (1987). The unusual conformation adopted by the adenine tracts in kinetoplast DNA. *Cell*, **48**, 935–943.

Chan, S. S., Breslauer, K. J., Austin, R. H. & Hogan, M. E. (1993). Thermodynamics and premelting conformational changes of phased $(dA)_5$ tracts. *Biochemistry*, **32**, 11776–11784.

Cheatham, T. E., III & Kollman, P. A. (1996). Observation of the *A*-DNA to *B*-DNA transition during unrestrained molecular dynamics in aqueous solution. *J. Mol. Biol.* **259**, 434–444.

Cheatham, T. E., III & Kollman, P. A. (1997). Molecular dynamics simulations highlight the structural differences among DNA:DNA, RNA:RNA and DNA:RNA hybrid duplexes. *J. Am. Chem. Soc.* **119**, 4805–4825.

Cheatham, T. E., III, Miller, J. L., Fox, T., Darden, T. A. & Kollman, P. A. (1995). Molecular dynamics simulations on solvated biomolecular systems: the particle mesh Ewald method leads to stable trajectories of DNA, RNA, and proteins. *J. Am. Chem. Soc.* **117**, 4193–4194.

Cheatham, T. E., III, Crowley, M. F., Fox, T. & Kollman, P. A. (1997). A molecular level picture of the stabilization of *A*-DNA in mixed ethanol-water solutions. *Proc. Natl Acad. Sci. USA,* **94**, 9626–9630.

Cornell, W. D., Cieplak, P., Bayly, C. I., Gould, I. R., Merz, K. M., Jr, Ferguson, D. M., Spellmeyer, D. C., Fox, T., Caldwell, J. W. & Kollman, P. A. (1995). A second generation force field for the simulation of proteins, nucleic acids, and organic molecules. *J. Am. Chem. Soc.* **117**, 5179–5197.

Crothers, D. M., Drak, J., Kahn, J. D. & Levene, S. D. (1992). DNA bending, flexibility, and helical repeat by cyclization kinetics. *Methods Enzymol.* **212**, 3–29.

Darden, T., York, D. & Pedersen, L. (1995). Particle mesh Ewald. *J. Chem. Phys.* **98**, 10089–10092.

Dickerson, R. E., Goodsell, D. S., Kopka, M. L. & Pjura, P. E. (1987). The effect of crystal packing on oligonucleotide double helix structure. *J. Biomol. Struct. Dynam.* **5**, 557–579.

Dickerson, R. E., Grzeskowiak, K., Grzeskowiak, M., Kopka, M. L., Larson, T., Lipanov, A., Prive, G. G., Quintana, J., Schultze, P., Yanagi, K., Yuan, H. & Yoon, H.-C. (1991). Polymophism, packing, resolution, and reliablity in single-crystal DNA oligomer analyses. *Nucleosides & Nucleotides,* **10**, 3–24.

Dickerson, R. E., Goodsell, D. & Kopka, M. L. (1996). MPD and DNA bending in crystals and in solution. *J. Mol. Biol.* **256**, 108–125.

Diekmann, S. (1987). Temperature and salt dependence of the gel migration anomaly of curved DNA fragments. *Nucl. Acids Res.* **15**, 247–265.

Diekmann, S. (1989). The migration anomaly of DNA fragments in polyacrylamide gels allows the detection of small sequence-specific DNA structure variations. *Electrophoresis,* **10**, 354–359.

Diekmann, S. & Wang, J. C. (1985). On the sequence determinants and flexibility of the kinetoplast DNA fragment with abnormal gel electrophoretic mobilities. *J. Mol. Biol.* **186**, 1–11.

DiGabriele, A. D., Sanderson, M. R. & Steitz, T. A. (1989). Crystal lattice packing is important in determining the bend of a DNA dodecamer containing an adenine tract. *Proc. Natl Acad. Sci. USA,* **86**, 1816–1820.

Duan, Y., Wilkosz, , Crowley, M. & Rosenberg, J. M. (1997). Molecular dynamics simulation study of DNA dodecamer d(CGCGAATTCGCG) in solution: conformation and hydration. *J. Mol. Biol.* **272**, 553–572.

Ferrin, T. E., Huang, C. C., Jarvis, L. E. & Langridge, R. (1988). The MIDAS display system. *J. Mol. Graph.* **6**, 13–27.

Flatters, D., Young, M. A., Beveridge, D. L. & Lavery, R. (1997). Conformational properties of the TATA box binding sequence of DNA. *J. Biomol. Struct. Dynam.* **14**, 1–8.

Fujimoto, B. S., Miller, J. M., Ribeiro, N. S. & Schurr, J. M. (1994). Effects of different cations on the hydrodynamic radius of DNA. *Biophys. J.* **67**, 304–308.

Ganunis, R. M., Guo, H. & Tullius, T. D. (1996). Effect of the crystallizing agent 2-methyl-2,4-pentanediol on the structure of adenine tract DNA in solution. *Biochemistry,* **35**, 13729–13732.

Gartenberg, M. R. & Crothers, D. M. (1991). Synthetic DNA bending sequences increase the rate of *in vitro* transcription initiation at the *Escherichia coli lac* promoter. *J. Mol. Biol.* **219**, 217–230.

Goodsell, D. S. & Dickerson, R. E. (1994). Bending and curvature calculations in *B*-DNA. *Nucl. Acids Res.* **22**, 5497–5503.

Hagerman, P. J. (1984). Evidence for the existence of stable curvature of DNA in solution. *Proc. Natl Acad. Sci. USA,* **81**, 4632–4636.

Hagerman, P. J. (1985). Sequence dependence of the curvature of DNA: a test of the phasing hypothesis. *Biochemistry,* **24**, 7033–7036.

Hagerman, P. J. (1990). Sequence-directed curvature of DNA. *Annu. Rev. Biochem.* **59**, 755–781.

Huang, C. C., Pettersen, E. F., Klein, T. E., Ferrin, T. E. & Langridge, R. (1991). Conic: a fast renderer for space-filling molecules with shadows. *J. Mol. Graph.* **9**, 230–236.

Hud, N. V. & Feigon, J. (1997). Localization of divalent metal ions in the minor groove of DNA *A*-tracts. *J. Am. Chem. Soc.* **119**, 5756–5757.

Impey, R. W., Madden, P. A. & McDonald, I. R. (1983). Hydration and mobility of ions in solution. *J. Phys. Chem.* **87**, 5071–5083.

Ioshikhes, I., Bolshoy, A. & Trifonov, E. N. (1992). Preferred positions of AA and TT dinucleotides in aligned nucleosomal DNA sequences. *J. Biomol. Struct. Dynam.* **9**, 1111–1117.

Jorgensen, W. L. (1981). Transferable intermolecular potential functions for water, alcohols and ethers. Application to liquid water. *J. Am. Chem. Soc.* **103**, 335–340.

Kim, J., Klooster, S. & Shapiro, D. J. (1995). Intrinsically bent DNA in a eukaryotic transcription factor recognition sequence potentiates transcription activation. *J. Biol. Chem.* **270**, 1282–1288.

Koo, H. S. & Crothers, D. M. (1988). Calibration of DNA curvature and a unified description of sequence-directed bending. *Proc. Nat. Acad. Sci. USA,* **85**, 1763–1767.

Koo, H. S., Drak, J., Rice, J. A. & Crothers, D. M. (1990). Determination of the extent of DNA bending by an adenine-thymine tract. *Biochemistry,* **29**, 4227–4234.

Lavery, R. & Sklenar, H. (1989). Defining the structure of irregular nucleic acids: conventions and principles. *J. Biomol. Struct. Dynam.* **6**, 655–667.

Lavery, R. & Sklenar, H. (1996). Curves 51: Helical analysis of irregular nucleic acids, edit. 5.1. Laboratoire de Biochimie Theorique, CNRS URA 77, Institut de Biologie Physico-Chimique, Paris, France.

Lavigne, M., Roux, P., Buc, H. & Schaeffer, F. (1997). DNA curvature controls termination of plus strand DNA synthesis at the centre of HIV-1 genome. *J. Mol. Biol.* **266**, 507–524.

Luger, K., Mader, A. W., Richmond, R. K., Sargent, D. F. & Richmond, T. J. (1997). Crystal structure of the nucleosome core particle at 2. 8 A resolution. *Nature,* **389**, 251–260.

Marini, J. C., Levene, S. D., Crothers, D. M. & Englund, P. T. (1982). Bent helical struture in kinetoplast DNA. *Proc. Natl Acad. Sci. USA,* **79**, 7664–7668.

Mehrotra, P. K. & Beveridge, D. L. (1980). Structural analysis of molecular solutions based on quasi-component distribution functions. Application to $[H_2CO]_{aq}$ at 25°C. *J. Am. Chem. Soc.* **102**, 4287–4294.

Mezei, M. & Beveridge, D. L. (1986). Structural chemistry of biomolecular hydration: the proximity criterion. *Methods Enzymol.* **127**, 21–47.

Miller, J. L. & Kollman, P. A. (1997). Theoretical studies of an exceptionally stable RNA tetraloop: observation of convergence from an incorrect NMR structure to the correct one using unrestrained molecular dynamics. *J. Mol. Biol.* **270**, 436–450.

Narayana, N., Ginell, S. L., Russu, I. M. & Berman, H. M. (1991). Crystal and molecular structure of a DNA fragment: d(CGTGAATTCACG). *Biochemistry,* **30**, 4449–4455.

Olson, W. K. & Zhurkin, V. B. (1996). Twenty years of DNA bending. In *Biological Structure and Dynamics* (Sarma, R. H. & Sarma, M. H., eds), pp. 341–370, Adenine Press, Albany, NY.

Olson, W. K., Marky, N. L., Jernigan, R. L. & Zhurkin, V. B. (1993). Influence of fluctuations on DNA curvature: a comparison of flexible and static wedge models of intrinsically bent DNA. *J. Mol. Biol.* **232**, 530–554.

Pearlman, D. A., Case, D. A., Caldwell, J. W., Ross, W. S., Cheatham, T. E., III, Fergusen, D. M., Seibel, G. L., Singh, U. C., Weiner, P. & Kollman, P. (1995). AMBER 4.1, edit 4.1. UCSF, San Francisco, CA.

Prevost, C., Louise, May S., Ravishanker, G., Lavery, R. & Beveridge, D. L. (1993). Persistence analysis of the static and dynamical helix deformations of DNA oligonucleotides: application to the crystal structure and molecular dynamics simulation of d(CGCGAATTCGCG)2. *Biopolymers,* **33**, 335–350.

Ravishanker, G. (1991). *Molecular Dynamics ToolChest 1.0 edit*., Wesleyan University, Middletown, CT.

Ravishanker, G., Swaminathan, S., Beveridge, D. L., Lavery, R. & Sklenar, H. (1989). Conformational and helicoidal analysis of 30 ps of molecular dynamics on the d(CGCGAATTCGCG) double helix: ''curves'', dials and windows. *J. Biomol. Struct. Dynam.* **6**, 669–699.

Saenger, W. (1983). *Principles of Nucleic Acid Structure*, Springer Verlag, New York.

Schellman, J. A. & Harvey, S. C. (1995). Static contributions to the persistence length of DNA and dynamic contributions to DNA curvature. *Biophys. Chem.* **55**, 95–114.

Shrader, T. E. & Crothers, D. M. (1990). Effects of DNA sequence and histone-histone interactions on nucleosome placement. *J. Mol. Biol.* **216**, 69–84.

Sinden, R. R. (1994). *DNA Structure and Function*, Academic Press, San Diego and London.

Sprous, D., Zacharias, W., Wood, Z. A. & Harvey, S. C. (1995). Dehydrating agents sharply reduce curvature in DNAs containing A-tracts. *Nucl. Acids Res.* **23**, 1816–1821.

Stofer, E. & Lavery, R. (1994). Measuring the geometry of DNA grooves. *Biopolymers,* **34**, 337–46.

Sundaralingam, M. & Sekharudu, Y. C. (1988). Sequence directed DNA bending and curvature. An overview. In *Structure and Expression* (Olson, W. K., Sarma, M. H., Sarma, R. H. & Sundaralingam, M., eds), pp. 9–23, Adenine Press, New York.

Trifonov, E. N. (1980). Sequence-dependent deformational anisotropy of chromatin DNA. *Nucl. Acids Res.* **8**, 4041–4053.

Tullius, T. D. & Burkhoff, A. M. (1988). Using the Chemistry of the hydroxyl radical to determine structural details of bent DNA. In *Structure and Expression* (Olson, W. K., Sarma, R. H., Sarma, R. H. & Sundaralingam, M., eds), vol. 3, pp. 77–85, Adenine Press, Albany, NY.

York, D. M., Wlodawer, A., Pedersen, L. G. & Darden, T. A. (1994). Atomic-level accuracy in simulations of large protein crystals. *Proc. Natl Acad. Sci. USA,* **91**, 8715–8718.

Young, M. A., Ravishanker, G., Beveridge, D. L. & Berman, H. M. (1995). Analysis of local helix bending in crystal structures of DNA oligonucleotides and DNA-protein complexes. *Biophys. J.* **68**, 2454–2468.

Young, M. A., Jayaram, B. & Beveridge, D. L. (1997a). Intrusion of counterions into the spine of hydration in the minor groove of *B*-DNA: fractional occupancy of electronegative pockets. *J. Am. Chem. Soc.* **119**, 59–69.

Young, M. A., Ravishanker, G. & Beveridge, D. L. (1997b). A 5-nanosecond molecular dynamics trajectory for *B*-DNA: analysis of structure, motions and solvation. *Biophys. J.* **73**, 2313–2336.

Zinkel, S. S. & Crothers, D. M. (1987). DNA bend direction by phase sensitive detection. *Nature,* **328**, 178–181.

Edited by B. Honig

(Received 28 January 1998; received in revised form 22 May 1998; accepted 26 May 1998)